

Beyond Periodic Orbits: An Example in Nonhydrogenic Atoms

P. A. Dando,¹ T. S. Monteiro,¹ D. Delande,² and K. T. Taylor³

¹*Department of Mathematics, Royal Holloway, University of London, Egham, Surrey, TW20 0EX, United Kingdom*

²*Laboratoire Kastler-Brossel, Université Pierre et Marie Curie, 4 place Jussieu, F-75005 Paris, France*

³*Department of Applied Mathematics and Theoretical Physics, Queen's University Belfast, Belfast, BT7 1NN, United Kingdom*

(Received 23 September 1994)

The spectrum of hydrogen in a magnetic field is a paradigm of quantum chaos and may be analyzed accurately by periodic-orbit-type theories. In nonhydrogenic atoms, the core induces pure quantum effects, especially additional spectral modulations, which cannot be analyzed reliably in terms of classical orbits and their stability parameters. Provided core-scattered waves are included consistently, core-scattered modulations as well as corrected amplitudes for primitive orbits are in excellent agreement with quantum results. We consider whether these systems correspond to quantum chaos.

PACS numbers: 05.45.+b, 03.65.Sq, 32.60.+i

Quantum chaos—the study of quantum systems associated with chaotic motion in the classical limit—continues to provide an important challenge to physics. One of the most dramatic correspondences between the quantum and classical mechanics of nonintegrable systems is contained in the so-called “periodic orbit expansion.” The simplest example is the Gutzwiller trace formula which expresses the quantum density of states (for a strongly chaotic system) as an infinite sum over periodic orbits of the classical system. This analysis relies on a semiclassical expansion of the Green’s function which is supposed to be valid for strongly chaotic systems and in the limit $\hbar \rightarrow 0$. In this Letter, we show—in the specific case of nonhydrogenic Rydberg states in a magnetic field—how the presence of a core induces pure quantum effects beyond the standard periodic (closed) orbit theory and how they can be successfully incorporated into the theory.

The highly excited hydrogen atom in a strong magnetic field has provided one of the most important case studies of a real quantum system for which the corresponding classical motion may be varied at will from regularity to chaos by adjusting a single parameter. The classical dynamics of the highly excited electron depends solely on one parameter, the scaled energy $\varepsilon = E\gamma^{-2/3}$ where γ is the magnetic field strength and E the energy. In atomic units the motion is almost fully regular for $\varepsilon < -0.5$ and makes a gradual transition, with increasing scaled energy, to full chaos for $\varepsilon > -0.127$ [1]. It is also possible to obtain quantum spectra corresponding to the same scaled energy, which may be compared with the classical dynamics. In this case, however, the scaling transformation results in an effective value of Planck’s constant equal to $\gamma^{1/3}$ [1].

The diamagnetic spectrum of hydrogen was analyzed quantitatively using periodic orbit theory [2] which was able to predict the positions and amplitudes of long-ranged modulations in the density of states. Similar modulations in the observed photoabsorption spectrum

have also been calculated using a theory [3–5] which involves closed rather than periodic orbits.

Now a growing body of experimental and theoretical evidence on spectra and wave-packet dynamics suggests that core effects have important dynamical effects not seen in hydrogen [6–8]. But the semiclassical theory routinely used to analyze experimental spectra neglects core effects entirely and hence is appropriate only for hydrogen [4].

Most theoretical quantum solutions of the diamagnetic nonhydrogenic problem [6,7,9] follow a suggestion of Clark and Taylor [10] who noted that the problem splits into two regions: an outer region where the core is negligible and the Hamiltonian is hydrogenic, and an inner region where the magnetic field is negligible. In the latter case the effect of the core is taken into account by a set of phase shifts dependent on angular momentum l —the quantum defects μ_l .

The first calculation on nonhydrogenic atoms at fixed scaled energies, permitting direct comparison with the classical dynamics, showed strong core-dependent effects [6]; additional modulations were found in Fourier-transformed spectra of nonhydrogenic atoms and the modulations of long-period orbits were reduced. The nearest neighbor statistics (NNS) were displaced towards the chaotic limit, even for low scaled energies ($\varepsilon = -0.5$) [6,11]. However, the quantum phase distributions showed that the eigenstates remain strongly localized on torus structures: not the signature of a true chaotic system. But unlike the regular limit where each quantum state is in general localized on a single torus, in this case each state receives contributions from different periodic and quasiperiodic trajectories.

Recently a method has been developed which enables calculation of nonhydrogenic spectra at fixed scaled energy for very high-lying states, closer to the semiclassical limit [7]. The additional modulations found in [6] were identified as being combinations of periodic orbits due to

core scattering. The fully quantal spectra presented below have also been calculated using this method.

A classical calculation [12] with a model potential which reproduces the quantum defects of lithium showed that, although typical trajectories are ergodic, when outside the core region (for $\varepsilon = -0.5$) they remained on a torus of hydrogen. Hence trajectories see all of phase space by "torus hopping," regular motion interspersed with scattering with the core. The periodic orbits have large Liapunov exponents, and the dynamics is extremely unstable. However, model-potential dynamics does not provide the true classical limit of core-scattering dynamics since the multielectron core affects only the lowest l -partial waves and so never approaches the semiclassical regime.

The only adequate approach must allow for the breakdown of classical path methods at the core. Closed-orbit theory [3–5] caters to this by matching a semiclassical wave approaching along a periodic orbit with a quantum scattered wave at the core boundary, $r = r_b$. The method is reviewed in [3,4] in great detail so only a very brief outline is given here. Du and Delos obtained the analytical form for the quantum scattering wave function

$$\Psi^j(r, \theta) = \psi_{\text{in}}^j(r, \theta) + \psi_{\text{out}}^j(r, \theta), \quad (1)$$

which arises when an electron approaches a core from an angle θ^j and includes an outgoing and an incoming part with amplitude N^j . The photoabsorption spectrum results from the overlap of these scattered waves with the initial wave produced by the photoabsorption process and consists of an average part plus an oscillatory part of the form

$$I(E) = -\frac{2(E - E_0)}{\pi} \text{Im} \sum_j N^j \langle D \phi_0 | \Psi^j \rangle. \quad (2)$$

Since the dipole matrix elements can be obtained from Coulomb functions, the important parameters are the amplitudes N^j of these scattered waves. They are determined by matching the ψ_{in}^j to semiclassical waves associated with periodic (closed) orbits:

$$\Phi_0(r_b, \theta_i^j) A^j e^{iS^j} = N^j \psi_{\text{in}}^j(r_b, \theta_f^j). \quad (3)$$

Here, j labels a closed orbit, which starts from the nucleus at an angle θ_i^j and returns some time later at an angle θ_f^j , and S^j corresponds to the action along that orbit plus an associated phase, the Maslov index. A^j is a semiclassical amplitude. The initial amplitude Φ_0 is determined by the photoabsorption process and is obtained [3] from the action of an outgoing Green's function on the dipole operator and the initial state. While the explicit dependence of Eq. (3) on r_b has been indicated, it has been shown [3] that the resulting solutions for the N^j 's are independent of r_b for small r_b .

After the encounter with the core, the scattered waves, ψ_{out}^j , launch other semiclassical waves along the same periodic orbits, so multiple traversals of these orbits

modulate the spectrum too. In the case of stable orbits the amplitudes oscillate with the number of traversals while for unstable orbits they decay exponentially.

It was noted [4] that only in the pure Coulomb case does ψ_{out}^j backscatter strongly into the same periodic orbit. In the presence of a nonzero quantum defect $\psi_{\text{out}}^j = \psi_{\text{Coul}}^j + \psi_{\text{core}}^j$. While ψ_{Coul}^j is strongly backwardly focused, ψ_{core}^j redistributes amplitude, isotropically for an $l = 0$ quantum defect or as $\cos\theta$ for p -wave scattering. Gao and Delos [4] investigated this process and concluded it was negligible.

It now seems amply clear that this is not generally the case [6–8,11]. One can estimate the amplitude of the additional observed core-scattered peaks perturbatively from ψ_{core}^j . However, this would not allow for loss of amplitude of the primary orbits.

Instead, we now consider that the initial outgoing wave consists not only of Φ_0 but in addition a coherent sum of core-scattered waves from all other closed orbits and their repetitions. Thus, in Eq. (3) we replace Φ_0 with $\tilde{\Phi}_0$ where

$$\tilde{\Phi}_0(r_b, \theta_i^j) = \Phi_0(r_b, \theta_i^j) + \sum_k N^k \psi_{\text{core}}^k(r_b, \theta_i^j) \quad (4)$$

and ψ_{core}^j is given by Eq. (7.14b) of Ref. [4]. The result is a set of coupled linear equations for the N^j 's; potentially, every orbit is coupled to every other by the scattering.

We solved this problem for $\varepsilon = -0.3$ using all primitive orbits (up to scaled action 6, 31 orbits in total) and their repetitions. The solutions were obtained by iteration. The first iteration returns the standard closed-orbit result: N^j is proportional to $A^j e^{iS^j}$. The second brings in combinations of two actions $A^j A^k e^{i(S^j + S^k)}$. The third brings in combinations of three primitive actions—double core scattering. And so on, until the results converge.

We find that the correction due to the p th iteration is weighted by a prefactor $\gamma^{p/6}$ or $\hbar^{p/2}$. Hence for small \hbar convergence with successive iterations is assured.

The same approach can also be used at values of ε where the hydrogenic classical motion is regular. In this case, the core scattering is seen to be the same mechanism as the torus hopping observed in the model-potential calculations.

In Figs. 1(a)–1(d) we compare the results for $m = 0$, odd l , and $\gamma^{-1/3} = 60$ –120. Figure 1(a) shows the Fourier-transformed spectrum of hydrogen. Figure 1(b) shows the quantum spectrum for an atom with $\mu_{l=1} = 0.5$ (comparable perhaps to Cs which has $\mu_{l=1} = 0.57$). Figure 1(c) shows the standard closed-orbit result with $\mu_{l=1} = 0.5$, while Fig. 1(d) shows the new version with the same quantum defect. One can see that, even for quite small values of \hbar ($n \approx 77$ –154), there is a substantial difference between hydrogen and the core-scattered case. Each peak in the Fourier transform is associated with a closed orbit. It appears at the action S^j of the orbit with an amplitude proportional to A^j . The core-scattered contributions are the peaks located at the sums $S^j + S^k$.

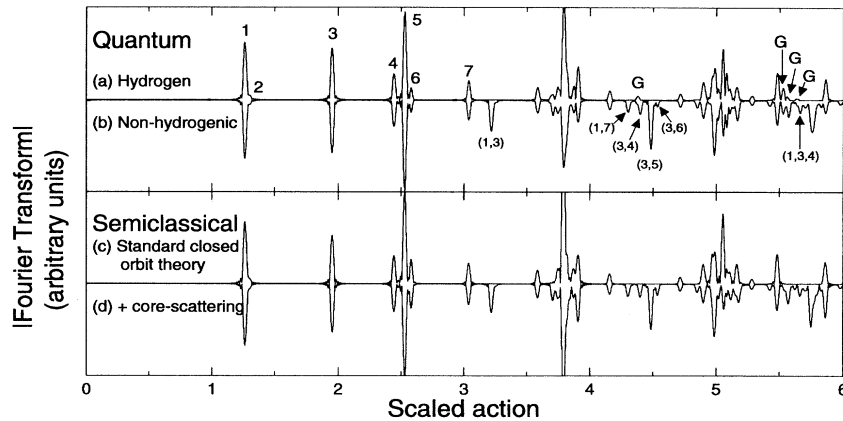


FIG. 1. Fourier transforms of the photoexcitation spectra (from the ground state) of Rydberg atoms in a magnetic field at constant scaled energy $\varepsilon = -0.3$ ($m = 0$, odd parity states, $\gamma^{-1/3}$ in the range 60–120). (a) Quantum result for hydrogen. The peaks appear at the actions of the closed orbits (see Table I for list). Also visible are ghost peaks (marked “G”). (b) Quantum results for a nonhydrogenic atom with $\mu_{l=1} = 0.5$; core-scattered peaks appear at the sum of actions of periodic orbits. (c) Standard semiclassical calculation for the hydrogen atom, in good agreement with (a), but not with (b). (d) Our semiclassical calculation, which goes beyond the standard closed-orbit theory by including core-scattering effects and successfully reproduces the quantum nonhydrogenic spectrum.

Further we can see that the standard closed-orbit result reproduces only the hydrogen results, while the new version with core scattering gives excellent agreement with the fully quantal nonhydrogenic case.

The integers in Fig. 1(a) indicate primary orbits. Table I gives the correspondence between these integers and the periodic orbits, following the convention of [13]. The pairs of integers in Fig. 1(b) indicate combinations of orbits, the core-scattered peaks. A few peaks present in Fig. 1(a) (indicated with a “G”) are not found even in the new semiclassical results. They correspond to “ghost” peaks [14], in other words, orbits which appear in the quantum spectrum below the energy of the bifurcation at which they are born. We have, in fact, identified a peak corresponding to scattering between a ghost and another “real” orbit. The triple integers indicate a peak due to double scattering, an action corresponding to a combination of three orbits. The Fourier transforms converged after two iterations, indicating that scattering beyond double scattering is unimportant. However, the difference between the first and second iterations was significant.

The major disagreement between the new semiclassical and the quantum results is in the peak for the third harmonic of V_1^1 . However, there is already a comparatively similar discrepancy for this peak between Figs. 1(a) and 1(c), the hydrogenic case. Such discrepancies occur when the semiclassical amplitude is near a singularity, for example, when a winding number is nearly rational. In that case the semiclassical result overestimates the quantum amplitude—the discrepancy increases for larger \hbar . Nevertheless, the new semiclassical results agree with the quantum in predicting a reduction of about 30% in amplitude of this peak due to core scattering. Very strong reductions in amplitudes of higher harmonics were seen in [6], which looked at very low-lying levels ($n \approx 10-30$)

where comparison with semiclassical results is more difficult.

Similarly, in Fig. 2 we compare the $\gamma^{-1/3} = 60-120$ range, this time for $m = 1$. Here photoabsorption excites, predominantly, states localized in the plane perpendicular to the magnetic field. Consequently, the Fourier transforms are dominated by the R_1 orbit and its harmonics, corresponding to periodic motion in a straight line perpendicular to the magnetic field. In the quantum hydrogenic [Fig. 2(a)] and also the standard closed orbit [Fig. 2(c)] spectrum the intensity of the harmonics alternates, with the even-numbered harmonics being stronger than the odd-numbered harmonics. At a nearby scaled energy $\varepsilon = -0.316$ the winding number ν of R_1 approaches a rational value, $\nu \approx 3/2$, and hence for even values of the number of traversals, k , the semiclassical amplitude $A \propto |\sin(\pi k \nu)|^{-1/2}$ diverges. In addition, the even- k peaks include contributions from the R_2^1 orbit born at $\varepsilon = -0.32$.

Once again we see that the new semiclassical results [Fig. 2(d)] are in much closer agreement with the quantum results [Fig. 2(b)] than the standard closed-orbit theory [Fig. 2(c)]. The additional core-scattered peaks are well reproduced. So are the amplitudes of the primary peaks which, particularly for higher scaled action, are significantly affected. The odd harmonics gain in amplitude, while some even ones lose amplitude. This we interpret as due to scattering between R_2^1 and R_1 which results in new peaks coincident with R_3 and R_5 . Ultimately, for high scaled action all strong harmonics have been lost. In [6] this was found to be a very strong effect indeed. We also found the reduction of amplitude of high harmonics to be more pronounced for $\gamma^{-1/3} = 30-60$ consistent with the \hbar dependence of core scattering. As in the $m = 0$ case, three iterations (terms up to a factor of \hbar)

TABLE I. Correspondence between the integers labeling the peaks in Fig. 1 and the periodic orbits described following the nomenclature of [13].

1	2	3	4	5	6	7
V_1^1	V_1	R_2^1	V_2^1	V_2^2	V_2	R_3^1

smaller than the standard periodic orbit form) were needed for convergence.

Loss of amplitude, which we find here for the higher harmonics, is characteristic of unstable motion. For true unstable motion the Liapunov exponents are positive producing semiclassical amplitudes which decay exponentially with the number of traversals. We have also found that these core-scattering systems can exhibit NNS statistics at the Wigner limit. The classical motion obtained from model-potential simulations is certainly chaotic. So may one conclude—even at low scaled energies where the hydrogenic dynamics is regular—that nonhydrogenic atoms represent another instance of quantum chaos.

Although the quantum modulations lose amplitude through core scattering, they do not do so exponentially. The results do not seem consistent with the large Liapunov exponents obtained for the closed orbits using the model potential, although recent calculations [15] suggest that clusters of new unstable orbits can explain some of the features observed in the quantum spectrum. In addition, the phase-space distributions are still concentrated on regular structures, though clearly they see much more of

phase space than a truly regular system in the regime of torus quantization. Finally, the core-scattering contributions decay with a higher power of \hbar than the hydrogenic motion.

However, we found here that the core-scattered terms make a very slow exit from the spectrum. We have shown that throughout much of the observed spectrum for $\varepsilon = -0.3$ (we have considered n up to 300) the effects for an atom like Cs or Sr remain strong. The long-range modulations in the spectrum of nonhydrogenic atoms in magnetic fields will tend to the hydrogenic ones in the semiclassical ($\hbar \rightarrow 0$) limit; the short-range behavior (e.g., NNS) is unclear but remains near the Wigner limit for the range considered here. But rather than invoking chaos, these features may be understood, even in the hydrogenic regular regime, in terms of regular motion plus quantum scattering.

This work has been supported in part by EPSRC and also by the British Council through the Alliance Programme. Laboratoire Kastler-Brossel is unité associée 18 au CNRS. CPU time on a Cray C98 has been provided by IDRIS.

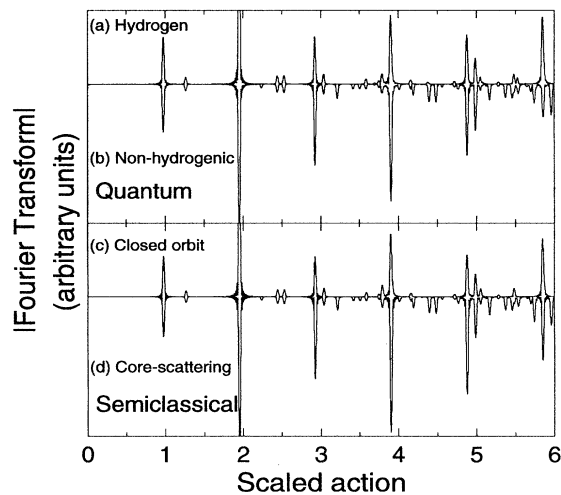


FIG. 2. Same as Fig. 1, but for $m = 1$ states. See text for discussion.

- [1] H. Hasegawa, M. Robnik, and G. Wunner, *Prog. Theor. Phys. Suppl.* **98**, 198 (1989).
- [2] D. Wintgen, *Phys. Rev. Lett.* **58**, 1589 (1987).
- [3] M. L. Du and J. B. Delos, *Phys. Rev. A* **38**, 1913 (1988).
- [4] J. Gao and J. B. Delos, *Phys. Rev. A* **46**, 1455 (1992).
- [5] E. B. Bogomolny, *Sov. Phys. JETP* **69**, 275 (1989); G. Alber, *Z. Phys. D* **14**, 307 (1989).
- [6] T. S. Monteiro and G. Wunner, *Phys. Rev. Lett.* **65**, 1100 (1990).
- [7] D. Delande *et al.*, *J. Phys. B* **27**, 2771 (1994).
- [8] G. Raithel, H. Held, L. Marmet, and H. Walther, *J. Phys. B* **27**, 2849 (1994); M. Courtney, H. Jiao, N. Spellmeyer, and D. Kleppner, *Phys. Rev. Lett.* **73**, 1340 (1994).
- [9] P. F. O'Mahony and K. T. Taylor, *Phys. Rev. Lett.* **57**, 2931 (1986); P. F. O'Mahony, *Phys. Rev. Lett.* **63**, 2653 (1989); M. H. Halley, D. Delande, and K. T. Taylor, *J. Phys. B* **26**, 1775 (1993).
- [10] C. W. Clark and K. T. Taylor, *J. Phys. B* **15**, 1175 (1982).
- [11] W. Jans, T. S. Monteiro, W. Schweizer, and P. A. Dando, *J. Phys. A* **26**, 3187 (1993).
- [12] P. A. Dando, T. S. Monteiro, W. Jans, and W. Schweizer, *Prog. Theor. Phys. Suppl.* **116**, 403 (1994).
- [13] A. Holle, J. Main, G. Wiebusch, H. Rottke, and K. H. Welge, *Phys. Rev. Lett.* **61**, 161 (1988).
- [14] M. Kuś, F. Haake, and D. Delande, *Phys. Rev. Lett.* **71**, 2167 (1993).
- [15] B. Hüpfer, J. Main, and G. Wunner (to be published).